

Oxidation Reactions Catalyzed by Polyoxomolybdate Salts

Bo Zhang^a, Su Li^a, Alexander Pöthig^a, Mirza Cokoja^a, Shu-Liang Zang^{b,c}, Wolfgang A. Herrmann^a, and Fritz E. Kühn^a

^a Chair of Inorganic Chemistry/Molecular Catalysis, Catalysis Research Center, Technische Universität München, Ernst-Otto-Fischer-Straße 1, D-85747 Garching bei München, Germany

^b School of Chemical and Materials Science, Liaoning Shihua University, Dandong Road, No.1, 113001 Fushun, P. R. China

^c Institute of Rare and Scattered Elements Chemistry, Liaoning University, Chongshan Middle Road No. 66, 110036 Shenyang, P. R. China

Reprint requests to Prof. W. A. Herrmann and Prof. F. E. Kühn. Tel: +49 89 289 13081. Fax: +49 89 289 13473. E-mail: wolfgangherrmann@ch.tum.de and fritz.kuehn@ch.tum.de

Z. Naturforsch. **2013**, *68b*, 587–597 / DOI: 10.5560/ZNB.2013-3033

Received January 30, 2013

Dedicated to Professor Heinrich Nöth on the occasion of his 85th birthday

Ionic compounds containing the polyoxomolybdate anion $[\text{Mo}_6\text{O}_{19}]^{2-}$ and $[(n\text{-C}_4\text{H}_9)_4\text{P}]^+$ (tetrabutylphosphonium), $[(n\text{-C}_4\text{H}_9)_3\text{P}(n\text{-C}_{14}\text{H}_{29})]^+$ (tributyl (tetradecyl)phosphonium), $[\text{Bmim}]^+$ (1-butyl-3-methylimidazolium) and $[\text{Dbmim}]^+$ (1,2-dimethyl-3-butylimidazolium) cations were prepared and characterized, including the determination of three of the solid state structures by single-crystal X-ray diffraction. These compounds were applied as catalysts for the epoxidation of olefins with urea hydrogen peroxide (UHP) as oxidant in the ionic liquid $[\text{Bmim}]\text{PF}_6$. Additionally, the oxidation of sulfides to sulfoxides with hydrogen peroxide (H_2O_2) in several solvents was investigated. The polyoxomolybdate catalysts showed a good performance for epoxidation of olefins as well as for oxidation of sulfides. Furthermore, the catalysts can be recycled several times in oxidation reactions. We present this methodology for the oxidation reaction in a simple, economically, technically, and environmentally benign manner.

Key words: Catalysis, Ionic Liquids, Molybdenum, Oxidation, Polyoxomolybdate, Epoxides, Sulfoxides

Introduction

Polyoxometalates (POMs) are an important and structurally diverse class of inorganic metal oxide clusters [1], which are not only used as inorganic components for novel materials, but also recognized as “green” industrial catalysts [2, 3]. Recently, ionic liquids (ILs) have received enormous attention in both academic and industrial research due to their unique physicochemical properties and the resulting applicability in various fields [4–10]. We and others have shown that certain anions exhibit an increased (catalytic) activity in ionic liquid media [11–14]. The concept of combining POM anions with “weakly coordinating cations” (WCC), such as those typically used for ionic liquids (tetraalkylammonium and -phosphonium, pyridinium,

imidazolium, and others), is thus regarded as a feasible way to increase the reactivity of POMs in ionic liquids. So far, some examples of WCC-POM compounds (*e. g.* $[\text{Bmim}]_3[\text{PW}_{12}\text{O}_{40}]$ ($\text{Bmim} = 1\text{-butyl-3-methylimidazolium}$), $[\text{Bmim}]_4[\text{SiM}_{12}\text{O}_{40}]$ and $[\text{Bmim}]_4[\text{S}_2\text{M}_{18}\text{O}_{62}]$ ($M = \text{Mo, W}$), $[(n\text{-C}_4\text{H}_9)_4\text{N}]_4[\text{Mo}_8\text{O}_{26}]$ and $[(n\text{-C}_4\text{H}_9)_4\text{N}]_2[\text{W}_6\text{O}_{19}]$) have been described and mainly used as electrochemicals [15–20]. However, only few POM salts have been investigated as catalysts. For example, the Keggin-type POM anion $[\text{PW}_{12}\text{O}_{40}]^{3-}$ can be used as catalyst for esterification [21] and for epoxidation reactions in ionic liquids [22]. The compound $[(n\text{-C}_4\text{H}_9)_4\text{N}]_2[\text{W}_6\text{O}_{19}]$ was found to be a catalyst for the synthesis of biscoumarins, which was investigated by Davoodna [23]. From these results it appears that tungsten-based WCC-POMs can exhibit excellent

catalytic performance because of controllable redox and acidic properties [24–26], which make them economical and environmentally acceptable. In contrast to tungsten-based WCC-POMs, which were widely used as catalysts for oxidation reactions, molybdenum-based congeners, such as the Lindqvist-type POM $[\text{Mo}_6\text{O}_{19}]^{2-}$, are rather rare and have not been often used in oxidation catalysis so far. The findings of our previous report on the catalytic oxidation of sulfides to sulfoxides using imidazolium tetrafluoroborate- and perrhenate-based ionic liquids using H_2O_2 [11–14] prompted us to investigate the catalytic properties of molybdenum-based WCC-POMs for the epoxidation of olefins and the selective oxidation of sulfides to sulfoxides.

The catalytic olefin epoxidation is of high importance in the chemical industry and also valuable for the synthesis of fine chemicals such as pharmaceuticals and flavor & fragrance components [27–30]. A vast number of coordination compounds have been applied as catalysts for this type of reaction [31–33]. However, the typical molecular transition metal catalysts are too expensive for a broad use and for upscaling, so that cheaper and recyclable catalysts are required. Organic sulfoxides are also important synthetic intermediates for the synthesis of various chemically and biologically active molecules [34–36]. Numerous reports on the oxidation of sulfides to sulfoxides using homogeneous transition metal catalysts in organic solvents have been published to date [37–45]. However, in most cases, the synthesis protocols involved formation of environmentally unfavorable by-products, and the catalysts are rather difficult to recycle and to separate from the products. We have now found that the above mentioned drawbacks can be overcome with WCC-POMs, confirming that they qualify as good catalyst for oxidation reactions.

In this work, we present the synthesis and characterization of a series of WCC-POMs containing tetrabutylphosphonium, tributyl(tetradecyl)phosphonium, 1-butyl-3-methylimidazolium, and 1-butyl-2,3-dimethylimidazolium cations along with the $[\text{Mo}_6\text{O}_{19}]^{2-}$ dianion, including three X-ray single-crystal structure determinations. The WCC-POMs show high stability and selectivity for epoxidation of olefins with anhydrous urea hydrogen peroxide (UHP) as oxidant in the ionic liquid $[\text{Bmim}]\text{PF}_6$. Additionally, a highly efficient method for selective oxidation of a series of sulfides to produce the corresponding sulfoxides in ex-

cellent yield using aqueous hydrogen peroxide as oxidant and WCC-POMs as catalyst under mild reaction conditions was also investigated. The WCC-POMs can be reused several times without significant loss of activity.

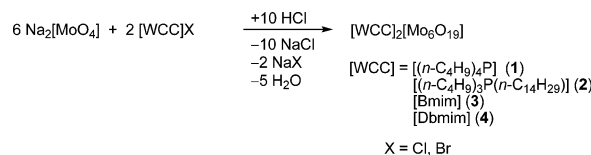
Results and Discussion

Synthesis of WCC-POMs

The WCC-[Mo₆O₁₉]²⁻ salts with [(n-C₄H₉)₄P] (1), [(n-C₄H₉)₃P(n-C₁₄H₂₉)] (2), [Bmim] (3) and [Bdmim] (4) cations were prepared by a modified literature procedure, which involves acid condensation in aqueous solution followed by addition of the precipitating cation (see Scheme 1) [46–48]. The success of the synthesis of WCC-POMs strongly depends on the pH of the reaction solution, the solvent and the temperature. The by-product (sodium halide) can easily be removed by extraction with water. Recrystallization was performed from acetonitrile. More detailed procedures are given in the Experimental Section. All synthesized WCC-POMs are very stable and can be handled on air. They are highly soluble in CH₃CN, but insoluble in water and methanol.

Characterization of the WCC-POM compounds **1–4**

Thermogravimetric analysis (TGA), differential scanning calorimetry (DSC) and IR spectroscopy data of compounds **1–4** are given in Table 1. TGA indicates that all four compounds show negligible volatility and high thermal stability with decomposition temperatures near 300 °C. $[(n\text{-C}_4\text{H}_9)_3\text{P}(\text{n-C}_{14}\text{H}_{29})_2][\text{Mo}_6\text{O}_{19}]$



Scheme 1. Synthesis of the WCC-POMs **1–4**.

Table 1. Melting points (T_m), decomposition temperatures (T_d) and characteristic IR data of compounds **1–4**.

Compound	T_m (°C)	T_d (°C)	IR (cm ⁻¹)			
1	196	341	949	920	791	720
2	68	338	950	914	785	718
3	128	290	961	908	801	741
4	193	293	948	902	787	754

(**2**) is the only compound which has a melting point below 100 °C (68 °C). The melting points of $[(n\text{-C}_4\text{H}_9)_4\text{P}]_2[\text{Mo}_6\text{O}_{19}]$ (**1**), $[\text{Bmim}]_2[\text{Mo}_6\text{O}_{19}]$ (**3**) and $[\text{Bdmim}]_2[\text{Mo}_6\text{O}_{19}]$ (**4**) are 196, 128 and 193 °C, respectively. Notably, the melting points of the phosphonium salts **1** and **2** decrease with increasing alkyl chain length from butyl to tetradecyl. The lower degree of crystal packing and long-range order, caused by the long alkyl chain in **2**, is most presumably the reason for the significantly different melting points of compounds **1** and **2**. The different melting points of compounds **3** and **4** are a consequence of the substitution of a proton in the 2-position of the imidazolium ring by a methyl group. A comparison of the structures of compounds **3** and **4** *via* Hirshfeld surface analysis [49, 50] revealed that in compound **4** the $[\text{Mo}_6\text{O}_{19}]^{2-}$ anions form more attractive contacts to the cations than in compound **3** (Supporting Information available online; see note at the end of the paper for availability). Furthermore, the degree of hydrogen-oxygen interactions in **4** is also higher, leading to a higher melting point.

IR spectroscopy was used to identify the structure of the $[\text{Mo}_6\text{O}_{19}]^{2-}$ anion. In the region of 700–1100 cm^{-1} , four characteristic bands at around 960 and 790 cm^{-1} are ascribed to $\nu(\text{Mo}-\text{O}_t)$ and $\nu(\text{Mo}-\text{O}_b-\text{Mo})$ modes of the $[\text{Mo}_6\text{O}_{19}]^{2-}$ anion (O_t and O_b mark terminal and bridging oxo ligands, respectively) [18, 51–53].

Crystal structures of WCC-POMs **1**, **3** and **4**

Crystals of the new compounds **1**, **3** and **4** were grown by slow evaporation of an acetonitrile solution at room temperature. Unfortunately, we were so far not able to obtain crystals of compound **2** of a quality suitable for single-crystal X-ray diffraction. The structures of compounds **1**, **3** and **4** reveal that the $[\text{Mo}_6\text{O}_{19}]^{2-}$ anion consists of six distorted MoO_6 octahedra which are connected by edges and a common vertex (Fig. 1) [54–56]. There are three types of oxygen atoms in the anion (terminal oxygen O_t , μ_2 -bridging oxygen O_b , and central oxygen O_c). Thus, the Mo–O bond lengths can be grouped into three sets (Table 2). Interestingly, the bond lengths Mo– O_b (1.8740(2)–1.967(1) Å) for **4** are longer than in the WCC-POMs **1** (1.868(1)–2.002(1) Å) and **3** (1.862(2)–2.015(2) Å), but the bond lengths Mo– O_t and Mo– O_c are similar. Further, a number of charge-assisted hydrogen bonds $\text{CH}\cdots\text{O}$ exist between the

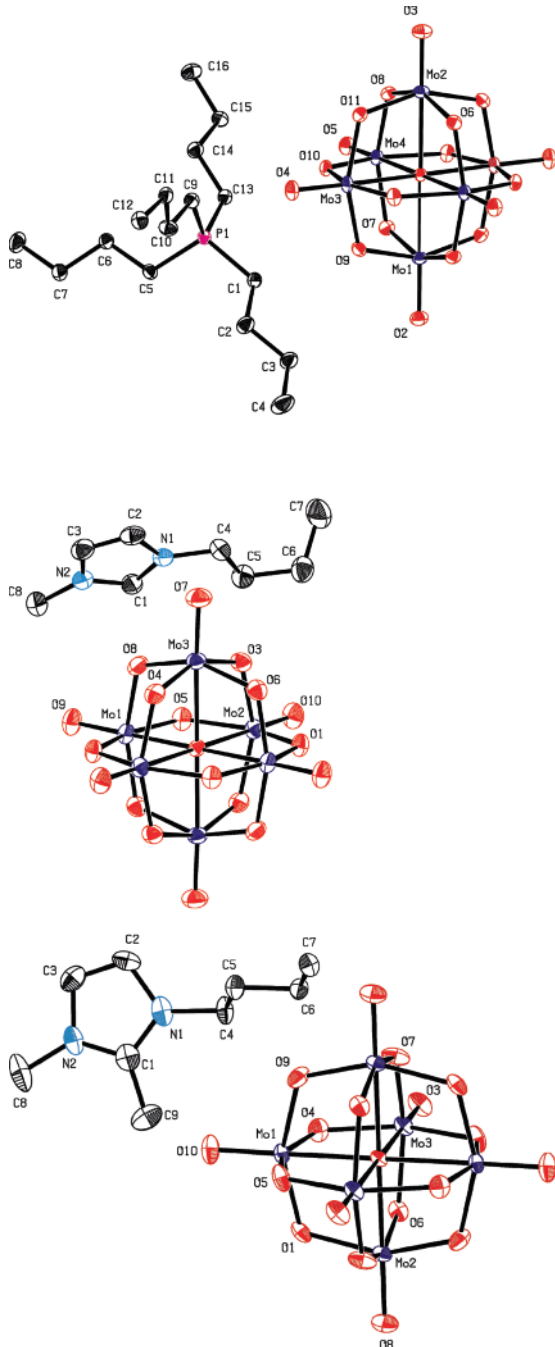


Fig. 1 (color online). ORTEP views of $[(n\text{-C}_4\text{H}_9)_4\text{P}]_2[\text{Mo}_6\text{O}_{19}]$ (**1**) (above, symmetry code: $-x, y, 1/2 - z$), $[\text{Bmim}]_2[\text{Mo}_6\text{O}_{19}]$ (**3**) (middle, symmetry code: $-x, y + 1/2, 1/2 - z$) and $[\text{Bdmim}]_2[\text{Mo}_6\text{O}_{19}]$ (**4**) (below, symmetry code: $1/2 - x, y + 1/2, 1/2 - z$) showing displacement ellipsoids at the 50% probability level. H atoms are omitted for clarity.

	1	3	4
Mo–O _t	1.672(2)–1.688(1)	1.678(2)–1.68(2)	1.6780(3)–1.686(1)
Mo–O _b	1.868(1)–2.002(1)	1.862(2)–2.015(2)	1.8740(2)–1.967(1)
Mo–O _c	2.313(2)–2.319(1)	2.318(1)–2.329(1)	2.3157(3)–2.324(1)

cation $-\text{CH}_n$ functions and the oxygen atoms of the anion $[\text{Mo}_6\text{O}_{19}]^{2-}$ (Fig. 1).

Each polyoxoanion is surrounded by $[(n\text{-C}_4\text{H}_9)_4\text{P}]$, $[\text{Bmim}]$ or $[\text{Bdmim}]$ cations, respectively, exhibiting $\text{H}\cdots\text{O}$ distances in the range of 2.254 to 2.680 (Å) for **1**, 2.493 to 2.665 (Å) for **3** and 2.358 to 2.680 (Å) for **4**, which indicate interactions between the polyoxoanions and the cations *via* Coulomb forces and $\text{CH}\cdots\text{O}$ hydrogen bonds. For compound **1**, contacts between the CH_2 and CH_3 groups of the butyl moieties and the $\text{O}(\text{O}_t, \text{O}_b)$ atoms of $[\text{Mo}_6\text{O}_{19}]^{2-}$ can be observed. Compounds **3** and **4** also exhibit contacts between the anion and the imidazolium ring hydrogen atoms and the alkyl substituents of the cation.

Catalytic epoxidation of olefins

Compounds **1**–**4** were examined as catalysts of the epoxidation of *cis*-cyclooctene. The organic and ionic liquid solvents, as well as the oxidants were varied in order to determine the optimum reaction conditions (Table 3). The yield of epoxide was indeed found to be strongly dependent on these parameter. Noteworthy, the (usually undesired) by-product 1,2-cyclooctanediol was not found in the entire set of experiments. The observed conversion was very low (< 30%) with CH_3CN and $[\text{Bmim}]\text{BF}_4$ as solvents (entries 1–2 and 4–6). On the other hand, when the reaction was carried out in methanol and in the ionic liquids $[\text{Bmim}]\text{PF}_6$ and $[\text{Bmim}]\text{NTf}_2$ (NTf_2 = bis(trifluoromethylsulfonyl)imide) as solvents, the yield of epoxide was significantly higher (entries 3, 7–9 and 11–13). The nature of the oxidant also plays a crucial role in the reaction. Three different oxidants [aqueous H_2O_2 , *tert*-butyl hydroperoxide (TBHP) in *n*-decane and urea-hydrogen peroxide (UHP)] were examined under comparable conditions. From the results shown in Table 3, entries 7–13, it can be stated that a) aqueous hydrogen peroxide solutions inhibit the catalytic reaction to some extent, and b) UHP is superior to both TBHP and H_2O_2 . Obviously, the olefin conversion significantly depends on the content of water in the solution. The catalytic reaction in the ionic liquid $[\text{Bmim}]\text{PF}_6$ with UHP ex-

Table 2. Selected bond lengths (Å) of **1**, **3** and **4**.

Table 3. Epoxidation of *cis*-cyclooctene with different oxidants and in different solvents at 60 °C using WCC-POM **1** as catalyst^a.

Entry	Solvent	Oxidant	Conv. (%) ^b	Yield (%) ^c
1	CH_3CN	H_2O_2 (35 %)	29	29
2	CH_3CN	TBHP	30	30
3	MeOH	H_2O_2 (35 %)	70	70
4	$[\text{Bmim}]\text{BF}_4$	H_2O_2 (35 %)	17	17
5	$[\text{Bmim}]\text{BF}_4$	TBHP	9	9
6	$[\text{Bmim}]\text{BF}_4$	UHP	9	9
7	$[\text{Bmim}]\text{PF}_6$	H_2O_2 (35 %)	49	49
8	$[\text{Bmim}]\text{PF}_6$	TBHP	69	69
9	$[\text{Bmim}]\text{PF}_6$	UHP	89	89
10	$[\text{Bmim}]\text{PF}_6$	—	—	—
11	$[\text{Bmim}]\text{NTf}_2$	H_2O_2 (35 %)	54	54
12	$[\text{Bmim}]\text{NTf}_2$	TBHP	56	56
13	$[\text{Bmim}]\text{NTf}_2$	UHP	63	63

^a Reaction conditions: *cis*-cyclooctene (2 mmol), catalyst **1** (1 mol-%), oxidant (4 mmol), solvent (1 mL), 60 °C, 4 h; ^b the conversion to cyclooctene oxide was determined by GC analysis; ^c the yield was determined by GC analysis.

hibited both a high yield of 89 % and a selectivity of > 99 % within 4 h (entry 9). Therefore, the usage of water-free UHP is crucial for successful epoxidation. Furthermore, in the blank experiments, no reaction occurred in the absence of oxidant UHP, indicating that the oxygen source of epoxides is not air (entry 10). Epoxidation of *cis*-cyclooctene at different temperatures was investigated as well. The reaction conditions were the same as those of entry 9 in Table 3.

As indicated in Fig. 2, a lower temperature was disadvantageous for the oxidation reaction. The yield was only 69 % within 4 h, and 72 % after 24 h at 50 °C. Because of the high yield (93 % within 4 h, 97 % after 24 h) at 70 °C, we chose 70 °C as the reaction temperature for further experiments.

Subsequently, in a comparative study the other synthesized WCC-POMs **2**–**4** were also used as catalysts in the epoxidation of *cis*-cyclooctene with UHP at 70 °C for 2 h. The results are shown in Table 4. Compound **3** exhibits the highest reactivity and conversion for the epoxidation of *cis*-cyclooctene (entry 3), most presumably due to the particularly high solubility in $[\text{Bmim}]\text{PF}_6$ at 70 °C. The other catalysts **1**, **2** and **4** also exhibited good results, and the yields were 93, 90 and 94 %, respectively (entries 1–2, 4).

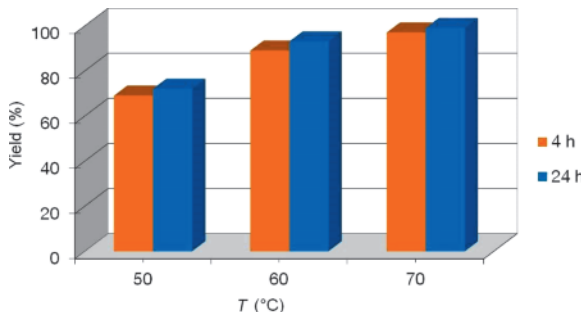


Fig. 2 (color online). Effect of temperature and reaction time for the catalytic epoxidation of *cis*-cyclooctene with compound **1** as catalyst. Reaction conditions: *cis*-cyclooctene (2 mmol), catalyst **1** (1 mol-%), UHP (4 mmol), [Bmim]PF₆ (1 mL).

Table 4. Epoxidation of *cis*-cyclooctene with different catalysts in [Bmim]PF₆ at 70 °C^a.

Entry	Catalyst	Conv. (%) ^b	Yield (%) ^c	TOF (h ⁻¹) ^d
1	1	93	93	47
2	2	90	90	45
3	3	97	97	49
4	4	94	94	47

^a Reaction conditions: *cis*-cyclooctene (2 mmol), catalyst (1 mol-%), UHP (4 mmol), [Bmim]PF₆ (1 mL), 70 °C, *t* = 2 h; ^b the conversion was determined by GC analysis; ^c the yield was determined by GC analysis; ^d determined after 2 h reaction time.

The catalyst recycling and reusability were studied as well. First, the product was extracted with *n*-hexane and the ionic liquid phase containing the catalyst was washed with water to remove urea ([Bmim]PF₆ and WCC-POMs are insoluble in water). The IL was then dried in high vacuum and used for the next catalytic run. The WCC-POMs remained active for at least three catalytic runs. However, a slight decrease of conversion and yield was observed (Fig. 3). Most presumably, this is resulting from the work-up procedure, since the IL catalyst solution is washed several times with *n*-hexane and thereafter with water. Hence, it is reasonable to assume that phase separation and subsequent decantation of the *n*-hexane and water phase might have led to unintentional extraction of small amounts of the IL.

Catalyst **3** was applied for the epoxidation of various olefins with UHP as oxidant (Table 5). Cyclohexene was readily converted into the epoxide within 1.5 h with 88 % yield (entry 2). Only moderate conversion (46 %) was observed for 1-octene (entry 3), which is less prone to epoxidation than *cis*-cyclooctene.

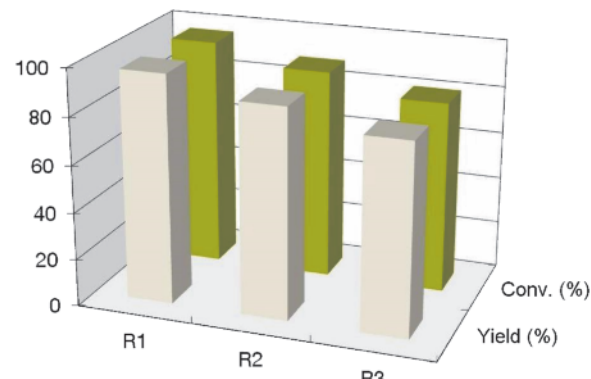


Fig. 3 (color online). Recycling studies of the IL catalyst mixture for the epoxidation of *cis*-cyclooctene.

The epoxidations of *trans*- β -methylstyrene (entry 4), limonene (entry 5), *cis*-stilbene (entry 6) and (+)-camphene (entry 7) were rather challenging due to steric hindrance (26 % after 3 h, 24 % after 7 h, 25 % after 4 h, 9 % after 8 h, respectively). The turnover frequencies (TOFs) are in the range of 16–182 h⁻¹. It is noteworthy that no diol is detected in all investigated reactions.

Selective catalytic oxidation of sulfides to sulfoxides

We investigated the oxidation reaction of thioanisole as a model substrate with different oxidants and in various solvents. The results are presented in Table 6 showing that the reaction was sensitive to the solvent. In *n*-hexane (entry 1), CH₂Cl₂ (entry 2) and water (entry 4) rather low conversions and yields were obtained due to the poor solubility of the catalyst in these solvents. When the reaction was carried out in acetonitrile (entry 3) high conversion (97 %) and yield (82 %) were obtained within 40 min, but the selectivity of sulfoxide was relatively lower than when using methanol, which was found to be a more efficient reaction medium (95 % yield, 97 % conversion, entry 5). Note that methanol itself can act as catalyst of the oxidation of thioanisole [57–59]. However, the reaction time is usually significantly longer (18 h), whereas in our experiments using catalyst **3** in methanol, high conversion (97 %) was reached already after 40 min (entry 5). The conversion was only 41 % without catalyst (entry 9).

Thus, it can safely be concluded that methanol is not catalyzing the oxidation in our case. The absence

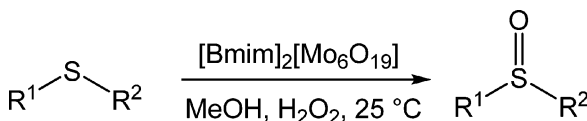
Table 5. Epoxidation of olefins with UHP catalyzed by **3** at 70 °C^a.

Entry	Substrate	Product	Time (h)	Conv. (%) ^b	Yield (%) ^c	TOF (h ⁻¹) ^d
1			2	97	97	148
2			1.5	88	88	182
3			4	46	46	30
4			3	26	26	48
5			7	24	24	16
6			4	25	25	32
7			8	9	9	—

^a Reaction conditions: *cis*-cyclooctene (2 mmol), **3** (1 mol-%), UHP (4 mmol), [Bmim]PF₆ (1 mL), 70 °C; ^b the conversion was determined by GC analysis; ^c the yield was determined by GC analysis; ^d determined after 15 min reaction time.

of oxidant leads to a significant decrease of conversion (28 %, entry 7). An obvious decrease of oxidation activity was observed by adding TBHP as oxidant (entry 6). The yield decreased to 46 % after 4 h without any solvent (entry 8).

In an effort to establish the scope of our protocol, a series of sulfides with different substituents were used (Scheme 2) in methanol. All oxidation reactions were performed under the same conditions (Table 7) and showed nearly quantitative conversions within a very short time (< 3 h). The sulfoxides were obtained



Scheme 2. Oxidation of sulfides to sulfoxides with aqueous hydrogen peroxide in methanol using [Bmim]₂[Mo₆O₁₉] (**3**) as catalyst.

in very good selectivities (> 80 %). TOFs were in the range of 165–380 h⁻¹.

Interestingly, sulfides with methyl groups (entry 1) were found to be more easily oxidized within short

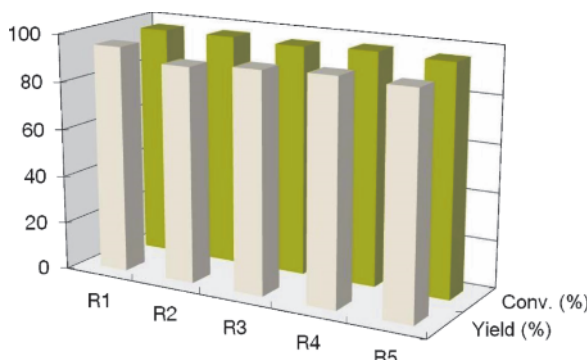
Table 6. Oxidation of thioanisole with different oxidants in different solvents at 25 °C^a.

Entry	Solvent	Oxidant	Time (h)	Conv. (%) ^b	Yield (%) ^c
1	<i>n</i> -hexane	H ₂ O ₂ (35 %)	4	82	57
2	CH ₂ Cl ₂	H ₂ O ₂ (35 %)	4	16	14
3	CH ₃ CN	H ₂ O ₂ (35 %)	0.67	97	82
4	H ₂ O	H ₂ O ₂ (35 %)	4	80	67
5	MeOH	H₂O₂ (35 %)	0.67	97	95
6	MeOH	TBHP	3	73	71
7	MeOH	—	24	28	27
8	—	H ₂ O ₂ (35 %)	4	93	46
9	MeOH	H ₂ O ₂ (35 %)	8	52 ^d	41

^a Reaction conditions: thioanisole (2 mmol), **3** (1 mol-%), H₂O₂ (35 %, 2.1 mmol), solvent (1 mL) 25 °C; ^b determined by GC on the crude reaction mixture; ^c isolated yield after column chromatogram.

time (*ca.* 30 min) compared to other substrates with bulky substituents, indicating that the steric hindrance is an important factor for the oxidation reaction. It was a significant observation that functional groups such as allyl (entry 6), hydroxo (entry 7) and ester moieties (entry 9) were not affected in this oxidation procedure. Noteworthy the WCC-POM catalyst **3** was very easily recovered by filtration when the reaction was completed. Therefore, the WCC-POMs-H₂O₂ system offered a facile, rapid and highly selective method to obtain sulfoxides.

The reusability of the catalyst WCC-POMs for oxidation of sulfides to sulfoxides was also studied. After the oxidation of thioanisole using **3** as catalyst was completed, ethyl acetate was added to the reaction mixture and the catalyst was precipitated, filtered, washed

Fig. 4 (color online). Recycling of the catalyst **3** in the oxidation of thioanisole with H₂O₂.

with ethyl acetate, and dried in vacuum at room temperature. Five catalytic runs were carried out and the results are shown in Fig. 4. It has to be noted that no significant loss of conversion and yield was observed after five runs, indicating a rather steady reusability of the WCC-POM catalyst. In comparison to the recycling of the IL catalyst mixture for the epoxidation of olefins, in this case the catalyst precipitation is a more convenient method to recover the catalyst without a loss after each cycle.

Conclusion

The epoxidation of olefins and the oxidation of sulfides to sulfoxides catalyzed by polyoxomolybdate salts containing weakly coordinating cations was achieved under mild conditions. The catalysts are eas-

Entry	R ¹	R ²	Time (min)	Conv. (%) ^b	Yield (%) ^c	TOF (h ⁻¹) ^d
1	Me	Me	30	96	95	190 ^e
2	<i>n</i> -Bu	<i>n</i> -Bu	40	96	94	141
3	Ph	Me	40	97	95	143
4	Ph	Et	40	93	92	138
5	Ph	CH(CH ₃) ₂	40	95	94	141
6	Ph	CH ₂ —CH=CH ₂	40	95	93	138
7	Ph	CH ₂ CH ₂ OH	45	90	87	125
8	Ph	CH ₂ OMe	60	88	87	120
9	Ph	CH ₂ COOMe	70	87	86	140
10	Ph	Ph	150	93	83	83
11	Ph	Bz ^f	70	90	85	98
12	Bz	Bz	60	89	86	110

^a Reaction conditions: thioanisole (2 mmol), **3** (1 mol-%), H₂O₂ (35 %, 2.1 mmol), MeOH (1 mL) at 25 °C; ^b determined by GC or ¹H NMR on the crude reaction mixture; ^c isolated yield after column chromatography; ^d TOFs of the catalyst were calculated over 40 min; ^e TOFs of the catalyst were calculated over 30 min; ^f Bz = benzyl.

Table 7. Oxidation of sulfides to sulfoxides with H₂O₂ as oxidant using **3** as catalyst in MeOH^a.

ily prepared, and can be recycled several times. The WCC-POM catalysts show high stability and selectivity for the epoxidation of olefins in the ionic liquid [Bmim]PF₆ with anhydrous urea hydrogen peroxide (UHP) as oxidant. For the selective oxidation of sulfides to the corresponding sulfoxides a method using aqueous hydrogen peroxide as oxidant has also been developed. Both catalytic reactions are cost-efficient.

Experimental Section

General methods

All reactions were performed using standard Schlenk techniques under an argon atmosphere. All solvents were collected from purification systems and kept over molecular sieves. ¹H NMR, ¹³C NMR and ³¹P NMR spectra were recorded on a Bruker Avance DPX-400 spectrometer. IR spectra were recorded on a Varian FTIR-670 spectrometer, using a GladiATR accessory with a diamond ATR element. Catalytic runs were monitored by GC methods on a Hewlett-Packard instrument HP 5890 Series II equipped with a FID, a Supelco column Alphadex 120 and a Hewlett-Packard integration unit HP 3396 Series II. Elemental analyses were performed with a Flash EA 1112 series elemental analyzer. Thermogravimetric (TG) and differential scanning calorimetric (DSC) analyses were conducted utilizing a Netzsch-STA 409 PC system. Typically about 10 mg of each sample was heated from 25 to 1000 °C at 10 K min⁻¹. Melting points were determined by MPM-H2 melting point meters. TLC was performed on silica gel 60F254 plates procured from E. Merck. Silica gel (0.06–0.2 mm 60 Å) was used for column chromatography. All chemicals were purchased from Acros and ABCR and used without further purification. [Bmim]PF₆, [Bmim]BF₄ and [Bmim]NTf₂ were synthesized according to literature procedures [60, 61].

Synthesis of [(n-C₄H₉)₃P(n-C₁₄H₂₉)₂]₂Mo₆O₁₉] (1)

Na₂MoO₄ · 2H₂O (4.8 g, 20 mmol) in H₂O (20 mL) was mixed with acetonitrile, and HCl (37%, 10 mL) was added. The resulting mixture was refluxed for 1 h. After cooling, the lower aqueous layer was discarded, and the upper layer was treated with [(n-C₄H₉)₃P]Br (2.7 g, 10.4 mmol) in water (100 mL). The precipitate was filtered and thoroughly washed successively three times with water and ethanol. Recrystallization of the solid from acetonitrile afforded yellow crystals of [(n-C₄H₉)₃P]₂Mo₆O₁₉. – IR (cm⁻¹): ν = 434.9 (s), 594.8 (m), 720.6 (m), 920.2 (w), 949.0 (vs), 1003.8 (w), 1100.9 (w), 1085.4 (w), 1378.8 (w), 1462.5 (w), 1919.5 (w), 2157.9 (w), 2871.1 (w), 2929.5 (w), 2959.6 (w). – ¹H NMR (400 MHz, [D₆]DMSO, r.t., ppm): δ = 0.93 (d, 12H), 1.42

(m, 16H), 2.19 (m, 8H) ³¹P NMR (162 MHz, [D₆]DMSO, r.t., ppm): δ = 33.78. – Elemental analysis (%): calcd. C 27.48, H 5.19; found C 27.55, H 5.20.

Synthesis of [(n-C₄H₉)₃P(n-C₁₄H₂₉)₂]₂Mo₆O₁₉] (2)

Na₂MoO₄ · 2H₂O (4.8 g, 20 mmol) in H₂O (20 mL) was mixed with acetonitrile, and HCl (37%, 10 mL) was added. The resulting mixture was refluxed for 1 h. After cooling, the lower aqueous layer was discarded, and the upper layer was treated with [(n-C₄H₉)₃P(n-C₁₄H₂₉)₂]Cl (4.99 g, 10.4 mmol) in water (100 mL). The precipitate was filtered and thoroughly washed successively three times with water and ethanol. Recrystallization of the solid from acetonitrile afforded pale-green crystals of [(n-C₄H₉)₃P(n-C₁₄H₂₉)₂]₂Mo₆O₁₉. – IR (cm⁻¹): ν = 436.3 (s), 591.4 (s), 718.9 (w), 785.5 (vs), 914.6 (w), 950.2 (vs), 1098.6 (w), 1459.6 (m), 1902.5 (w), 2850.2 (m), 2920.2 (m), 2956 (w). – ¹H NMR (400 MHz, [D₆]DMSO, r.t., ppm): δ = 0.89 (d, 3H), 1.00 (d, 9H), 1.29 (m, 18H), 1.39 (d, 2H), 1.56 (m, 8H), 1.70 (m, 8H), 2.40 (m, 8H). – ³¹P NMR (162 MHz, [D₆]DMSO, r.t., ppm): δ = 33.95. – Elemental analysis (%): calcd. C 37.15, H 6.84; found C 36.67, H 6.43.

Synthesis of [Bmim]₂Mo₆O₁₉] (3)

Na₂MoO₄ · 2H₂O (4.8 g, 20 mmol) was dissolved in 10 mL H₂O, and an aqueous solution of HCl (37%, 5 mL) was added. After stirring for 10 min, [Bmim]Br (1.6 g, 3.75 mmol) was added with vigorous stirring. The precipitate was filtered and thoroughly washed successively three times with water and ethanol. Recrystallization of the solid from acetonitrile afforded yellow crystals of [Bmim]₂Mo₆O₁₉. – IR (cm⁻¹): ν = 437.1 (m), 614.5 (m), 753.6 (s), 786.2 (vs), 878.6 (w), 911.8 (m), 952.3 (vs), 1164.3 (m), 1462.0 (w), 1568.3 (w), 1906.3 (w), 2870.2 (w), 2930.9 (w), 2959.3 (w), 3115.6 (w), 3144.8 (w). – ¹H NMR (400 MHz, [D₆]DMSO, r.t., ppm): δ = 0.91 (d, 3H), 1.27 (m, 2H), 1.78 (m, 2H), 3.87 (s, 3H), 4.17 (t, 2H), 7.69 (s, 1H), 7.75 (s, 1H), 9.10 (s, 1H) – ¹³C NMR (100 MHz, [D₆]DMSO, r.t., ppm): δ = 13.76, 19.28, 31.87, 36.23, 49.04, 122.70, 124.08, 136.95. – Elemental analysis (%): calcd. C 16.57, H 2.78, N 4.83; found C 16.69, H 2.61, N 4.64.

Synthesis of [Bdmim]₂Mo₆O₁₉] (4)

Na₂MoO₄ · 2H₂O (4.8 g, 20 mmol) was dissolved in 10 mL H₂O, and an aqueous solution of HCl (37%, 5 mL) was added. After stirring for 10 min, [Bdmim]Br (1.75 g, 3.75 mmol) was added with vigorous stirring. The precipitate was filtered and thoroughly washed successively three times with water and ethanol. Recrystallization of the solid from acetonitrile afforded pale-yellow crystals of [Bdmim]₂Mo₆O₁₉. – IR (cm⁻¹): ν = 434.3 (s), 592.2 (s), 753.7 (s), 787.0 (vs), 948.6 (vs), 1093.2 (w), 1133.9 (w),

1247.0 (w), 1417.3 (w), 15334.6 (w), 1588.1 (w), 1901.0 (w), 2962.2 (w), 3140.6 (w). – ^1H NMR (400 MHz, $[\text{D}_6]\text{DMSO}$, r.t., ppm): δ = 0.92 (t, 3H), 1.29 (m, 2H), 1.70 (m, 2H), 2.59 (s, 3H), 3.76 (s, 3H), 4.11 (t, 2H), 7.61 (s, 1H), 7.64 (s, 1H) – ^{13}C NMR (100 MHz, $[\text{D}_6]\text{DMSO}$, r.t., ppm): δ = 9.60, 13.87, 19.37, 31.64, 35.14, 47.79, 121.32, 122.78, 144.64. – Elemental analysis (%): calcd. C 18.20, H 3.05, N 4.72; found C 18.14, H 2.94, N 4.65.

General procedure for the epoxidation of olefins

In a typical reaction, the catalyst (20 μmol) was dissolved in solvent (1 mL). Substrate (2 mmol) was added, followed by the addition of UHP (4 mmol, 0.3762 g). The reaction mixture was extracted with *n*-hexane (5 \times 1 mL) and then monitored by quantitative GC analysis. Samples were taken at regular time intervals. The resulting slurry was filtered and the filtrate injected onto a GC column. The conversion of olefins and the formation of epoxides were calculated from calibration curves ($r^2 > 0.999$) recorded prior to the reaction. For the recycling experiment, 3 mL of water was added to the mixtures after extracting the substrate and the product with *n*-hexane. The upper phase was removed from the reaction by means of cannulation. The IL phase was washed three times with water and then dried in vacuum for 4 h. Fresh substrate and UHP were then added for a new reaction cycle.

General procedure for the oxidation of sulfides

Catalyst (20 μmol) and sulfide (2 mmol) were dissolved in MeOH (1 mL), followed by dropwise addition of H_2O_2 (35%) (0.19 mL, 2.1 mmol) at room temperature. The progress of the reaction was followed by TLC. After completion of the reaction, 3 mL of ethyl acetate was added to the mixture to obtain the catalyst by filtration. The solvent was removed under vacuum for 4 h and then the crude products were analyzed by GLC or ^1H NMR using internal standard technology. The sulfoxides were purified by column chromatography (silica gel using hexane-ethyl acetate 90 : 10 v/v). For the recycling experiment, ethyl acetate was added to the reaction mixture after the reaction was completed and the catalyst precipitated, filtered off, washed with ethyl acetate, and dried in high vacuum at room temperature. All products were characterized by melting point, ^1H NMR, ^{13}C NMR and IR spectroscopy (see Supporting Information).

Single-crystal X-ray structure determinations

The data were collected on an X-ray diffractometer equipped with a CCD detector (APEX II, κ -CCD), a rotating anode (Bruker AXS, FR591) or a fine-focused sealed tube with MoK_α radiation ($\lambda = 0.71073 \text{ \AA}$), and a graphite monochromator by using the SMART software package [62]. The measurements were performed on single crystals coated with Paratone oil and mounted on glass capillaries. Each

crystal was frozen under a stream of nitrogen. A matrix scan using at least 20 centered reflections was used to determine the initial lattice parameters. Reflections were merged and corrected for Lorentz and polarization effects, scan speed, and background using SAINT [62]. Absorption corrections, including odd and even ordered spherical harmonics were performed using SADABS [63]. Space group assignments were based upon systematic absences, E statistics, and successful refinement of the structures. Structures were solved using Bruker APEX suite [64], and were refined with all data using SHELXLE [65, 66]. Hydrogen atoms were assigned idealized positions and refined using a riding model with an isotropic displacement parameter 1.2 times that of the attached carbon atom (1.5 times for methyl hydrogen atoms). If not mentioned otherwise, non-hydrogen atoms were refined with anisotropic displacement parameters. Full-matrix least-squares refinements were carried out by minimizing $\Sigma w(F_o^2 - F_c^2)^2$ with the SHELXL-97 weighting scheme [67], [68]. Neutral atom scattering factors for all atoms and anomalous dispersion corrections for the non-hydrogen atoms were taken from International Tables for Crystallography [69]. Images of the crystal structures were generated by PLATON [70, 71] and Mercury [72, 73].

1: pale-yellow fragment, $2(\text{C}_{16}\text{H}_{36}\text{P})\text{-Mo}_6\text{O}_{19}$, $M_r = 1398.48$, monoclinic, space group $C2/c$ (no. 15), $a = 16.0547(3)$, $b = 16.0680(3)$, $c = 19.7281(4) \text{ \AA}$, $\beta = 106.248(1)^\circ$, $V = 4885.94(16) \text{ \AA}^3$, $Z = 4$, $\lambda(\text{Mo}K_\alpha) = 0.71073 \text{ \AA}$, $\mu = 1.6 \text{ mm}^{-1}$, $\rho_{\text{calcd.}} = 1.90 \text{ g cm}^{-3}$, $T = 123(1) \text{ K}$, $F(000) = 2792$, $\theta_{\text{max}} = 25.44^\circ$, $R_1 = 0.0156$ (4133 observed data), $wR_2 = 0.0370$ (all 4475 data), GOF = 1.053, 414 parameters, $\Delta\rho_{\text{max/min}} = 0.34 / -0.34 \text{ e \AA}^{-3}$.

3: light-yellow fragment, $2(\text{C}_8\text{H}_{15}\text{N}_2)\text{-Mo}_6\text{O}_{19}$, $M_r = 1158.08$, monoclinic, space group $P2_1/c$ (no. 14), $a = 8.546(2)$, $b = 17.085(3)$, $c = 11.075(2) \text{ \AA}$, $\beta = 106.248(1)^\circ$, $V = 1529.5(5) \text{ \AA}^3$, $Z = 2$, $\lambda(\text{Mo}K_\alpha) = 0.71073 \text{ \AA}$, $\mu = 2.5 \text{ mm}^{-1}$, $\rho_{\text{calcd.}} = 2.52 \text{ g cm}^{-3}$, $T = 123(1) \text{ K}$, $F(000) = 1116$, $\theta_{\text{max}} = 25.62^\circ$, $R_1 = 0.0165$ (2584 observed data), $wR_2 = 0.0395$ (all 2836 data), GOF = 1.064, 208 parameters, $\Delta\rho_{\text{max/min}} = 0.34 / -0.27 \text{ e \AA}^{-3}$.

4: light-yellow fragment, $2(\text{C}_9\text{H}_{17}\text{N}_2)\text{-Mo}_6\text{O}_{19}$, $M_r = 1186.13$, monoclinic, space group $P2_1/n$ (no. 14), $a = 11.0074(2)$, $b = 10.7827(2)$, $c = 13.5900(3) \text{ \AA}$, $\beta = 91.045(1)^\circ$, $V = 1612.72(5) \text{ \AA}^3$, $Z = 2$, $\lambda(\text{Mo}K_\alpha) = 0.71073 \text{ \AA}$, $\mu = 2.3 \text{ mm}^{-1}$, $\rho_{\text{calcd.}} = 2.44 \text{ g cm}^{-3}$, $T = 123(1) \text{ K}$, $F(000) = 1148$, $\theta_{\text{max}} = 25.47^\circ$, $R_1 = 0.0256$ (2902 observed data), $wR_2 = 0.0660$ (all 2989 data), GOF = 1.161, 218 parameters, $\Delta\rho_{\text{max/min}} = 1.36 / -0.58 \text{ e \AA}^{-3}$.

For more detailed information on all crystal structure determinations, see the Supporting Information.

CCDC 892238 ($[(n\text{-C}_4\text{H}_9)_4\text{P}]_2[\text{Mo}_6\text{O}_{19}]$), CCDC 892239 ($[\text{Bmim}]_2[\text{Mo}_6\text{O}_{19}]$), and CCDC 892240 ($[\text{Bdmim}]_2[\text{Mo}_6\text{O}_{19}]$) contain the supplementary crys-

tallographic data for this paper. These data can be obtained free of charge from The Cambridge Crystallographic Data Centre *via* www.ccdc.cam.ac.uk/data_request/cif.

are given as Supporting Information available online (DOI: [10.5560/ZNB.2013-3033](https://doi.org/10.5560/ZNB.2013-3033)).

Acknowledgement

B. Z. thanks the TUM Graduate School for financial support. S.-L. Z. thanks the National Natural Science Foundation of China (21071073) and the Cooperation Project (21111130584) for the financial support.

Supporting information

Detailed information on all crystal structure determinations and spectroscopic data characterizing the sulfoxides

- [1] P. G. Rickert, M. R. Antonio, M. A. Firestone, K. Kubatko, T. Szreder, J. F. Wishart, M. L. Dietz, *J. Phys. Chem. B* **2007**, *111*, 4685–4692.
- [2] I. V. Kozhevnikov, *Chem. Rev.* **1998**, *98*, 171–198.
- [3] L. C. W. Baker, D. C. Glick, *Chem. Rev.* **1998**, *98*, 3–49.
- [4] J. P. Hallett, T. Welton, *Chem. Rev.* **2011**, *111*, 3508–3576.
- [5] R. Giernoth, *Angew. Chem. Int. Ed.* **2010**, *49*, 2834–2849.
- [6] S. G. Lee, *Chem. Commun.* **2006**, 1049–1063.
- [7] P. Wasserscheid, W. Keim, *Angew. Chem. Int. Ed.* **2000**, *39*, 3772–3789.
- [8] V. I. Pârvulescu, C. Hardacre, *Chem. Rev.* **2007**, *107*, 2615–2665.
- [9] F. V. Rantwijk, R. A. Sheldon, *Chem. Rev.* **2007**, *107*, 2757–2785.
- [10] P. Hapiot, C. Lagrost, *Chem. Rev.* **2008**, *108*, 2238–2264.
- [11] I. I. E. Markovits, W. A. Eger, S. Yue, M. Cokoja, B. Zhang, C. Münchmeyer, M.-D. Zhou, A. Genest, J. Mink, S.-L. Zang, N. Rösch, F. E. Kühn, *Chem. Eur. J.* **2013**, *19*, 5972–5979.
- [12] B. Zhang, S. Li, S. Yue, M. Cokoja, M. D. Zhou, S. L. Zang, F. E. Kühn, accepted for publication.
- [13] B. Zhang, M. D. Zhou, M. Cokoja, J. Mink, S. L. Zang, F. E. Kühn, *RSC Adv.* **2012**, *2*, 8416–8420.
- [14] E. A. Pidko, V. Degirmenci, E. J. M. Hensen, *Chem-CatChem* **2012**, *4*, 1263–1271.
- [15] M. H. Chang, J. A. Dzielawa, M. L. Dietz, M. R. Antonio, *J. Electroanal. Chem.* **2004**, *567*, 77–84.
- [16] J. Zhang, A. M. Bond, D. R. MacFarlane, S. A. Bond, A. G. Wedd, *Inorg. Chem.* **2005**, *44*, 5123–5132.
- [17] A. W. A. Mariotti, J. L. Xie, B. F. Abrahams, A. M. Bond, A. G. Wedd, *Inorg. Chem.* **2007**, *46*, 2530–2540.
- [18] T. Rajkumar, G. R. Rao, *Mater. Lett.* **2008**, *62*, 4134–4136.
- [19] T. Rajkumar, G. R. Rao, *Mater. Chem. Phys.* **2008**, *112*, 853–857.
- [20] T. Rajkumar, G. R. Rao, *Solid State Sci.* **2009**, *11*, 36–42.
- [21] Y. Leng, J. Wang, D. Zhu, X. Ren, H. Ge, L. Shen, *Angew. Chem. Int. Ed.* **2009**, *48*, 168–171.
- [22] L. Liu, C. Chen, X. Hu, T. Mohamood, W. Ma, J. Lin, J. Zhao, *New J. Chem.* **2008**, *32*, 283–289.
- [23] A. Davoodna, *Bull. Korean Chem. Soc.* **2011**, *32*, 4286–4290.
- [24] N. Mizuno, M. Misono, *Chem. Rev.* **1998**, *98*, 199–217.
- [25] M. Misono, *Chem. Commun.* **2001**, 1141–1152.
- [26] P. Zhao, M. Zhang, Y. Wu, J. Wang, *Ind. Eng. Chem. Res.* **2012**, *51*, 6641–6647.
- [27] S. A. Hauser, M. Cokoja, F. E. Kühn, *Catal. Sci. Technol.* **2013**, *3*, 552–561.
- [28] M. Herbert, F. Montilla, R. Moyano, A. Pastor, E. Álvarez, A. Galindo, *Polyhedron* **2009**, *28*, 3929–3934.
- [29] N. Gharah, S. Chakraborty, A. K. Mukherjee, R. Bhattacharyya, *Chem. Commun.* **2004**, 2630–2632.
- [30] M. Herbert, E. Álvarez, D. J. Cole-Hamilton, F. Montilla, A. Galindo, *Chem. Commun.* **2010**, *46*, 5933–5935.
- [31] D. Betz, A. Raith, M. Cokoja, F. E. Kühn, *ChemSusChem* **2010**, *3*, 559–562.
- [32] W. A. Herrmann, R. W. Fischer, D. W. Marz, *Angew. Chem., Int. Ed. Engl.* **1991**, *30*, 1638–1641.
- [33] M. Zhou, J. Zhao, J. Li, S. Yue, C. Bao, J. Mink, S. Zang, F. E. Kühn, *Chem. Eur. J.* **2007**, *13*, 158–166.
- [34] A. A. Lindén, M. Johansson, N. Hermanns, J.-E. Bäckvall, *J. Org. Chem.* **2006**, *71*, 3849–3853.
- [35] E. Baciocchi, M. F. Gerini, A. Lapi, *J. Org. Chem.* **2004**, *69*, 3586–3589.
- [36] E. Baciocchi, C. Chiappe, T. D. Giacco, C. Fasciani, O. Lanzalunga, A. Lapi, B. Melai, *Org. Lett.* **2009**, *11*, 1413–1416.
- [37] A. V. Anisimov, E. V. Fedorova, A. Z. Lesnugin, V. M. Senyavi, L. A. Aslanov, V. B. Rybakov, A. V. Tarakanova, *Catal. Today* **2003**, *78*, 319–325.
- [38] V. Conte, F. Fabbianesi, B. Floris, P. Galloni, D. Sordi, I. W. C. E. Arends, M. Bonchio, D. Rehder, D. Bogdal, *Pure Appl. Chem.* **2009**, *81*, 1265–1277.
- [39] G. P. Romanelli, D. O. Bennardi, V. Palermo, P. G. Vázquez, P. Tundo, *Lett. Org. Chem.* **2007**, *4*, 544–549.
- [40] J. H. Espenson, *Chem. Commun.* **1999**, 479–488.

[41] K. J. Stanger, J. W. Wiench, M. Pruski, J. H. Espenson, G. A. Kraus, R. J. Angelici, *J. Mol. Catal. A: Chem.* **2006**, *243*, 158–169.

[42] J. Legros, C. Bolm, *Angew. Chem. Int. Ed.* **2003**, *42*, 5487–5489.

[43] J. Legros, C. Bolm, *Angew. Chem. Int. Ed.* **2004**, *43*, 4225–4228.

[44] K. Jeyakumar, D. K. Chand, *Tetrahedron Lett.* **2006**, *47*, 4573–4576.

[45] M. Ciclosi, C. Dinoi, L. Gonsalvi, M. Peruzzini, E. Manoury, R. Poli, *Organometallics* **2008**, *27*, 2281–2286.

[46] D. L. Long, P. Kögerler, L. Cronin, *Angew. Chem. Int. Ed.* **2004**, *43*, 1817–1820.

[47] A. Thakur, A. Chakraborty, V. Ramkumar, S. Ghosh, *Dalton Trans.* **2009**, 7552–7558.

[48] D. L. Long, R. Tsunashima, L. Cronin, *Angew. Chem. Int. Ed.* **2010**, *49*, 1736–1758.

[49] M. A. Speckerman, D. Jayatilaka, *CrystEngComm* **2009**, *11*, 19–32.

[50] F. L. Hirshfeld, *Theor. Chim. Acta* **1977**, *44*, 129–138.

[51] S. Gatard, S. Blanchard, B. Schollhorn, P. Gouzerh, A. Proust, K. Boubekeur, *Chem. Eur. J.* **2010**, *16*, 8390–8399.

[52] M. Schulz-Dobrick, M. Jansen, *Z. Anorg. Allg. Chem.* **2007**, *633*, 2326–2331.

[53] T. Rajkumar, G. R. Rao, *J. Chem. Sci.* **2008**, *120*, 587–594.

[54] Y. Gao, X. Wang, Y. Li, E. Wang, L. Xu, C. Hu, *J. Coord. Chem.* **2004**, *57*, 445–451.

[55] V. Shivaiah, S. K. Das, *Angew. Chem. Int. Ed.* **2006**, *45*, 245–248.

[56] X. Ma, Z. Yang, C. Schulzke, *Z. Kristallogr.* **2010**, 775–776.

[57] K. Kaczorowska, Z. Kolarska, K. Mitka, P. Kowalski, *Tetrahedron* **2005**, *61*, 8315–8327.

[58] J. Drabowicz, M. Mikolajczyk, *Synth. Commun.* **1981**, *11*, 1025–1030.

[59] W. L. Xu, Y. Z. Li, Q. S. Zhang, H. S. Zhu, *Synthesis* **2004**, 227–232.

[60] J. G. Huddleston, A. E. Visser, W. M. Reichert, H. D. Willauer, G. A. Broker, R. D. Rogers, *Green Chem.* **2001**, *3*, 156–164.

[61] S. Park, R. J. Kazlauskas, *J. Org. Chem.* **2001**, *66*, 8395–8401.

[62] SMART, SAINT (version 7.56a), Area Detector Control and Integration Software, Bruker Analytical X-ray Instruments Inc., Madison, Wisconsin (USA) **2008**.

[63] SADABS (version 2008/1), Bruker Analytical X-ray Instruments Inc., Madison, Wisconsin (USA) **2008**.

[64] APEX 2 (version 2008.4), Suite of crystallographic software, Bruker Analytical X-ray Instruments Inc., Madison, Wisconsin (USA) **2008**.

[65] C. B. Hübschle, G. M. Sheldrick, B. Dittrich, SHELXLE, A Qt graphical user interface for SHELXL, University of Göttingen, Göttingen (Germany) **2011**.

[66] C. B. Hübschle, G. M. Sheldrick, B. Dittrich, *J. Appl. Cryst.* **2011**, *44*, 1281–1284.

[67] G. M. Sheldrick, SHELXL-97, Program for the Refinement of Crystal Structures, University of Göttingen, Göttingen (Germany) **1997**.

[68] G. M. Sheldrick, *Acta Crystallogr.* **2008**, *A64*, 112–122.

[69] A. J. C. Wilson (Ed.), *International Tables for Crystallography*, Vol. C, Kluwer Academic Publishers, Dordrecht **1992**; Tables 6.1.1.4 (pp. 500–502), 4.2.6.8 (pp. 219–222), and 4.2.4.2 (pp. 193–199).

[70] A. L. Spek, PLATON, A Multipurpose Crystallographic Tool, Utrecht University, Utrecht (The Netherlands) **2010**.

[71] A. L. Spek, *J. Appl. Crystallogr.* **2009**, *D65*, 148–155.

[72] C. F. Macrae, I. J. Bruno, J. A. Chisholm, P. R. Edgington, P. McCabe, E. Pidcock, L. Rodriguez-Monge, R. Taylor, J. van de Streek, P. A. Wood, MERCURY CSD 2.0, New features for the visualization and investigation of crystal structures, Cambridge Structural Database (CSD), Cambridge (U. K.) **2008**.

[73] C. F. Macrae, I. J. Bruno, J. A. Chisholm, P. R. Edgington, P. McCabe, E. Pidcock, L. Rodriguez-Monge, R. Taylor, J. van de Streek, P. A. Wood, *J. Appl. Crystallogr.* **2008**, *41*, 466–470.